Hydrophobic Polyelectrolytes

ARTICLE *in* MACROMOLECULES · FEBRUARY 1999

Impact Factor: 5.8 · DOI: 10.1021/ma981412j

2 AUTHORS:

Andrey V Dobrynin
University of Akron
124 PUBLICATIONS **4,912** CITATIONS
SEE PROFILE

Michael Rubinstein
University of North Carolina at Chapel Hill
103 PUBLICATIONS **4,899** CITATIONS
SEE PROFILE

Hydrophobic Polyelectrolytes

Andrey V. Dobrynin and Michael Rubinstein*

Department of Chemistry, University of North Carolina, Chapel Hill, North Carolina 27599-3290

Received September 8, 1998; Revised Manuscript Received November 5, 1998

ABSTRACT: We present a scaling model of hydrophobic polyelectrolytes. In dilute salt-free solutions these polymers have a necklacelike shape with compact beads joined by narrow strings. This necklacelike structure manifests itself in the unique scaling laws in semidilute regime for the concentration range where the correlation length ξ of a solution is on the order of the string length between two neighboring beads. In this regime the correlation length ξ decreases with polymer concentration c as $\xi \sim c^{-1/3}$, viscosity is concentration independent, and self-diffusion coefficient D increases with concentration $D \sim c^{1/3}$ in both unentangled and entangled solutions. The effects of added salt on the properties of hydrophobic polyelectrolyte solutions are also discussed.

1. Introduction

Polyelectrolytes[1,2]—polymers with charged groups have attracted much attention during the past three decades due to their unique properties and technological importance. One of the most important property of the polyelectrolytes is that they are water solvable. Many synthetic polymers do not dissolve in water due to hydrophobic interactions between hydrocarbon backbone and water molecules. These hydrophobic interactions cause chains without charged groups to collapse into spherical globules, coalesce with each other, and precipitate from the solution. Addition of the charged groups to polymer chains significantly improves their solubility in aqueous solutions.

The shape of hydrophobic polyelectrolytes in water is determined by the interplay between electrostatic and hydrophobic interactions. The problem of the shape of a charged globule is similar to the classical problem of the instability of a charged droplet, considered by Lord Rayleigh.[3] He showed that a charged droplet is unstable and breaks into smaller droplets if the electric charge exceeds some critical value. In equilibrium these smaller droplets (with the charge on each of them less than the critical one) are at an infinite distance from each other. This final state is impossible for a single charged polymer because it consists of monomers connected to each other by chemical bonds. In this case, the system reduces its energy by spliting into a set of smaller charged globules connected by narrow strings—the necklace globule.[4−6] In section 2.2 below, we describe this necklace conformation. In section 2.3, we discuss how this necklacelike structure of hydrophobic polyelectrolytes affects the static and dynamics properties of the salt-free semidilute solutions. We find that in addition to the usual regime expected for hydrophilic polyelectrolytes[12] there is a new regime with the correlation length of solution of the order of the length of the strings between neighboring beads. In this new semidilute regime the correlation length ξ decreases with increasing concentration c as $\xi \sim c^{-1/3}$ leading to unusual rheological properties. In section 3, we extend our model to semidilute solutions with higher concentration of salt. In section 4, we discuss the effects of counterion condensation, and in section 5, we compare the predictions of our model with experiments.

2. Salt-Free Solutions

2.1. Neutral Spherical Globules. Consider a dilute solution of chains with degree of polymerization N, monomer size b, and fraction of the charged monomers f in a poor solvent with dielectric constant ϵ. An uncharged chain in a poor solvent forms a globule.[7−9] The monomer density ρ inside this globule is defined by the balance between the two body attraction $-\tau b^3 \rho N$ and three-body repulsion $b^6 \rho^2 N$ leading to density

$$\rho \approx \tau / b^3 \tag{2.1}$$

where the reduced temperature is given by

$$\tau = (\Theta - T)/\Theta \tag{2.2}$$

and Θ is the theta temperature of the polymer. Note that in eq 2.1 and throughout the paper we drop numerical coefficients and keep our discussion at the scaling level. The size R of the globule with the average monomer density ρ is equal to

$$\mathrm{R} \approx (N/\rho)^{1/3} \approx b\tau^{-1/3} N^{1/3} \tag{2.3}$$

The density fluctuations inside the globule are suppressed on the length scales larger than the correlation length ξ_T (thermal blob size). On length scales smaller than ξ_T, the chain statistics is a random walk of g_T monomers ($\xi_T \approx b g_T^{1/2}$). On length scales larger than the thermal blob size ξ_T, the attraction between monomers forces the blobs to densely fill the volume of the globule $\rho \approx g_T/\xi_T^3$. The size of the thermal blob scales with the reduced temperature as

$$\xi_T \approx b/\tau \tag{2.4}$$

The surface tension γ of the globule is on the order of the thermal energy kT per thermal blob at the surface of a globule

$$\gamma \approx kT\xi_T^{-2} \approx kT\tau^2/b^2 \tag{2.5}$$

2.2. Charged Necklace Globules.[6] If the polymer is charged, the electrostatic interactions between charged monomers will change the shape of a globule but will not significantly affect its volume. As in the case of an uncharged polymer, the occupied volume is still defined

10.1021/ma981412j CCC: $18.00
Published on Web 01/21/1999

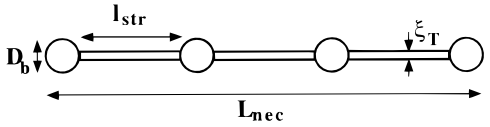

Figure 1. Sketch of a necklace globule. Each bead is of size D_b and contains m_b monomers. Each string is of length l_{str} and thickness ξ_T and contains m_{str} monomers.

by the solvent quality. A charged globule will spontaneously deform if the energy of the electrostatic repulsion between charges $F_{Coul} \approx e^2f^2N^2/\epsilon R$ becomes comparable to its surface energy $F_{surf} \approx kTR^2\xi_T^{-2}$. This deformation occurs when the total valence of the charge fN becomes larger than $(N\tau/u)^{1/2}$. Here the dimensionless interaction parameter

$$u = l_B/b \tag{2.6}$$

is the ratio of the Bjerrum length

$$l_B \approx e^2/\epsilon kT \tag{2.7}$$

to the bond size b.

For the higher charge densities $f > (\tau/uN)^{1/2}$ the polyelectrolyte globule will split into a set of smaller charged globules (beads) connected by narrow strings—the necklace globule (see Figure 1).[6] The size of the beads

$$D_b \approx b(uf^2)^{-1/3} \tag{2.8}$$

is determined by the Rayleigh stability condition $e^2f^2m_b^2/\epsilon D_b \approx kTD_b^2\xi_T^{-2}$, where

$$m_b \approx \tau/uf^2 \tag{2.9}$$

is the number of monomers in a bead ($m_b \approx \rho D_b^3$). The diameter of the strings is of the order of thermal blob size ξ_T (eq 2.4). The length l_{str} of a string connecting two beads can be estimated by balancing the electrostatic repulsion between two closest beads $kTl_Bf^2m_b^2/l_{str}$ and the surface energy of the string kTl_{str}/ξ_T. The equilibrium distance between beads is

$$l_{str} \approx b\left(\frac{\tau}{uf^2}\right)^{1/2} \approx bm_b^{1/2} \tag{2.10}$$

The mass of the string between neighboring beads $m_{str} \approx \rho l_{str}\xi_T^2$ is much smaller than the mass of the bead m_b

$$\frac{m_{str}}{m_b} \approx \left(\frac{uf^2}{\tau^3}\right)^{1/2} \ll 1 \tag{2.11}$$

In this case the number of beads N_{bead} on a chain is approximately equal to $N/m_b \approx uf^2N/\tau$. However, most of the length is stored in the strings ($l_{str} \gg D_b$); therefore, the length of the necklace is

$$L_{nec} \approx N_{bead}l_{str} \approx b\left(\frac{uf^2}{\tau}\right)^{1/2}N \approx b\frac{N}{m_b^{1/2}} \tag{2.12}$$

Below we develop a scaling model of semidilute solutions of hydrophobic polyelectrolytes based on the necklace model[6] reviewed above.

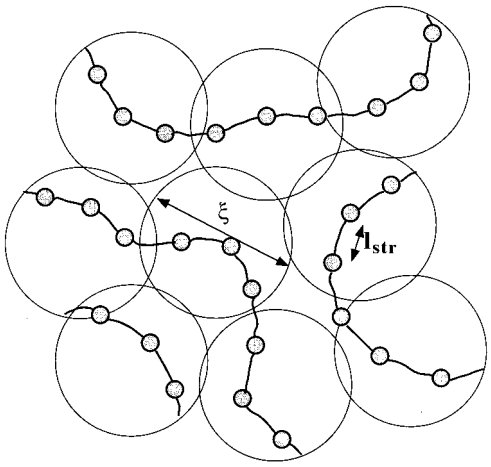

Figure 2. String-controlled semidilute solution ($c_0^* < c < c_b$) with correlation length ξ (eq 2.14) larger than string length l_{str} (eq 2.10).

2.3. Semidilute Solutions of Necklaces. 2.3.1. Static Properties. The crossover from dilute to semidilute solutions occurs at the overlap concentration

$$c_0^* \approx N/L_{nec}^3 \approx b^{-3}N^{-2}\left(\frac{\tau}{uf^2}\right)^{3/2} \approx \frac{m_b^{3/2}}{b^3N^2} \tag{2.13}$$

In a semidilute solution ($c > c_0^*$) the configuration of the chain on length scales shorter than the correlation length ξ is similar to that in dilute solutions (see Figure 2). On length scales longer than the correlation length ξ, the chain is assumed to be a random walk of correlation segments ξ. The correlation length at the overlap concentration $\xi(c_0^*)$ is equal to the necklace size L_{nec} and in the semidilute regime ($c > c_0^*$) is independent of the degree of polymerization[10−12]

$$\xi \approx L_{nec}\left(\frac{c_0^*}{c}\right)^{1/2} \approx b\left(\frac{\tau}{uf^2}\right)^{1/4}(cb^3)^{-1/2} \approx bm_b^{1/4}(cb^3)^{-1/2} \tag{2.14}$$

The correlation length is inversely proportional to the square root of polymer concentration.[10] The number of monomers in the correlation volume is

$$g \approx c\xi^3 \approx m_b^{3/4}(cb^3)^{-1/2} \tag{2.15}$$

The normal dependence of the correlation length ξ on polymer concentration (eq 2.14) continues as long as the correlation length ξ is larger than the length of the string l_{str} between neighboring beads. These two lengths become of the same order of magnitude ($\xi \approx l_{str}$) at polymer concentration

$$c_b \approx b^{-3}\left(\frac{uf^2}{\tau}\right)^{1/2} \approx b^{-3}m_b^{-1/2} \tag{2.16}$$

For higher polymer concentrations $c > c_b$ the electrostatic interaction between beads is screened, and we expect one bead per every correlation volume ξ^3 (see Figure 3).

The correlation volumes ξ^3 are space filling $c \approx g\xi^{-3}$. The number of monomers inside the correlation volume for $c > c_b$ is

$$g \approx c\xi^3 \approx m_b \tag{2.17}$$

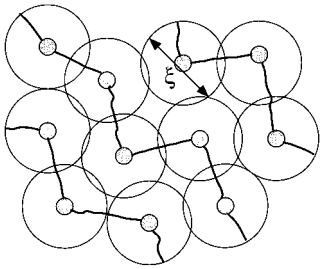

Figure 3. Bead-controlled semidilute solution ($c_b < c < c_D$) with correlation length ξ (eq 2.18) of the order of the distance between beads.

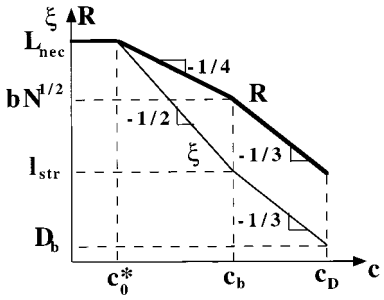

Figure 4. Concentration dependences of the correlation length ξ (thin line) and chain size R (thick line) in string-controlled ($c_0^* < c < c_b$) and bead-controlled ($c_b < c < c_D$) semidilute regimes. Both axes are logarithmic.

since we have assumed that most of the polymer mass is in beads (eq 2.11). Therefore the correlation length decreases inversely proportional to the one third power of polymer concentration (see Figure 4)

$$\xi \approx \left(\frac{\tau}{uf^2}\right)^{1/3} c^{-1/3} \approx \left(\frac{m_b}{c}\right)^{1/3} \tag{2.18}$$

This concentration dependence of the correlation length ξ is unusual for the semidilute solutions of polymers and is more typical for the distance between chains in dilute solutions (the system behaves as a dilute solution of beads).

Since the electrostatic interactions are screened on the length scales longer than the correlation length ξ, the configuration of a polyelectrolyte chain is that of a random walk of size (see Figure 4)

$$R \approx \xi\left(\frac{N}{g}\right)^{1/2} \approx bN^{1/2}\begin{cases}(c_b/c)^{1/4}, & c_0^* < c < c_b\\ (c_b/c)^{1/3}, & c_b < c < c_D\end{cases} \tag{2.19}$$

where c_D is the polymer concentrations at which the beads start to overlap. This crossover concentration is on the order of the concentration ρ inside the beads (eq 2.1)

$$c_D \approx \frac{m_b}{D_b^3} \approx \frac{\tau}{b^3} \approx \rho \tag{2.20}$$

Note that at the crossover between semidilute low-salt string-controlled (SLS) and bead-controlled (SLB) regimes (at $c \approx c_b$) the chain size is approximately Gaussian $R \approx bN^{1/2}$ but its configuration is not.

Below we will investigate the effect of the new concentration dependence of the correlation length (eq 2.18) and chain size (eq 2.19) on the dynamics of semidilute solutions.

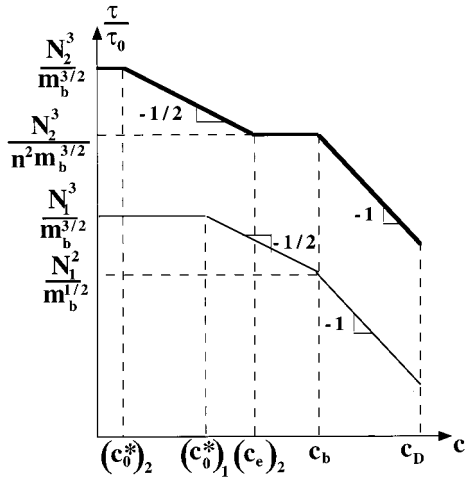

Figure 5. Concentration dependences of the relaxation time τ for unentangled (thin line) and entangled (thick line) semidilute solutions. Subscripts 1 and 2 refer to chains with degrees of polymerization N_1 and N_2 ($N_1 < m_b n^2 < N_2$). Both axes are logarithmic.

2.3.2. Dynamic Properties. The hydrodynamic interactions between different subsections of the chain control its dynamics on length scales shorter than the correlation length ξ. The motion on these length scales is Zimm-like. The relaxation time of the chain sections of the size of the correlation length ξ is

$$\tau_\xi \approx \eta_s \xi^3/kT \tag{2.21}$$

where η_s is the solvent viscosity. The hydrodynamic interactions are screened on the length scales longer than the correlation length ξ. The polyelectrolyte chain in an unentangled solution behaves as a Rouse chain of N/g effective monomers (correlation volumes) with the longest relaxation time

$$\tau \approx \tau_\xi\left(\frac{N}{g}\right)^2 \approx \frac{\eta_s b^3}{kT}\frac{N^2}{m_b^{1/2}}\begin{cases}(c_b/c)^{1/2}, & c_0^* < c < c_b\\ c_b/c, & c_b < c < c_D\end{cases} \tag{2.22}$$

The relaxation time decreases with concentration in both semidilute regimes. In the string-controlled regime ($c < c_b$) we recover the "normal" polyelectrolyte behavior[10−12] with the relaxation time decreasing as the square root of concentration $\tau \sim 1/\sqrt{c}$. In the new bead-controlled regime ($c > c_b$) the decrease of relaxation time is faster $\tau \sim 1/c$ (see Figure 5).

The self-diffusion coefficient is proportional to the ratio of mean square chain size (eq 2.19) and characteristic time (eq 2.22)

$$D \approx \frac{R^2}{\tau} \approx \frac{kT}{\eta_s b}\frac{m_b^{1/2}}{N}\begin{cases}1, & c < c_b\\ (c/c_b)^{1/3}, & c_b < c < c_D\end{cases} \tag{2.23}$$

The self-diffusion coefficient is constant in the unentangled string-controlled regime[11,12] and increases with concentration in the bead-controlled regime (Figure 6). This unusual increase is the result of the strongly decreasing relaxation time $\tau \sim 1/c$ (eq 2.22). The physical meaning of this increase is that the friction coefficient of chains in this bead-controlled regime is the sum over the same concentration-independent number of friction centers. The friction coefficient of each center is linearly

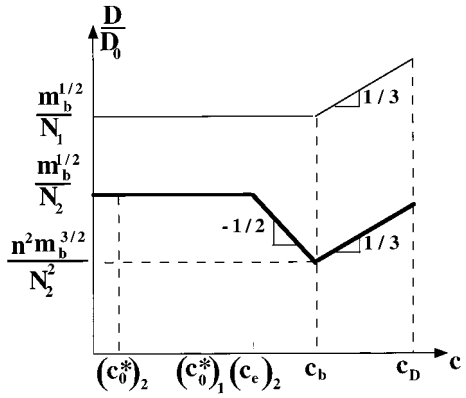

Figure 6. Concentration dependences of the self-diffusion coefficient D for unentangled (thin line) and entangled (thick line) semidilute solutions. Subscipts 1 and 2 refer to chains with degrees of polymerization N_1 and N_2 ($N_1 < m_b n^2 < N_2$). Both axes are logarithmic.

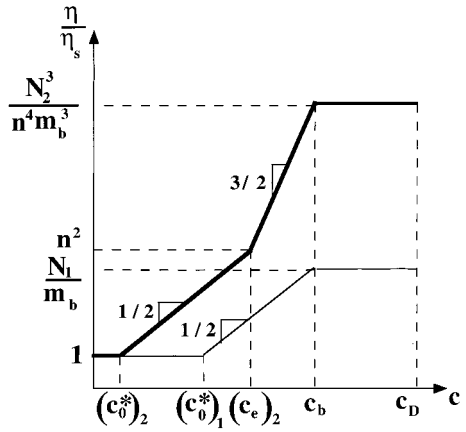

Figure 7. Concentration dependences of the viscosity η for unentangled (thin line) and entangled (thick line) semidilute solutions. Subscipts 1 and 2 refer to chains with degrees of polymerization N_1 and N_2 ($N_1 < m_b n^2 < N_2$). Both axes are logarithmic.

proportional to the correlation length ξ. Therefore the self-diffusion coefficient $D \sim 1/\xi$.

The modulus G of the unentangled solution is of the order of the thermal energy kT per chain. The viscosity in this semidilute unentangled regime is

$$\eta \approx G\tau \approx \eta_s \frac{N}{m_b}\begin{cases}(c/c_b)^{1/2}, & c_0^* < c < c_b \\ 1, & c_b < c < c_D\end{cases} \quad (2.24)$$

We recover the Fuoss law in the string-controlled semidilute regime[11,12] but predict a concentration independent viscosity in the bead-controlled semidilute unentangled regime $\eta \approx \eta_s N/m_b$ (Figure 7).

Above the entanglement concentration c_e the topological interactions dominate at distance scales larger than the tube diameter a. This distance scale can be defined so that there are always n strands of different chains[13,14] inside the entanglement volume a^3 where n is a constant of order 5−10. One can show that the diameter of a tube $a \approx n\xi$ and the degree of polymerization between entanglements is $N_e \approx n^2 g$. The longest relaxation time in the entangled regime can be estimated from the reptation model. Assuming polyelectrolyte dynamics to be Zimm-like up to the correlation length ξ, Rouse-like for a strand of $N_e/g \approx n^2$ correlation volumes of size ξ, and reptation-like for N/N_e entanglement strands, we can write for the longest relaxation time of entangled solutions of hydrophobic polyelectrolytes

$$\tau \approx \tau_\xi \left(\frac{N_e}{g}\right)^2 \left(\frac{N}{N_e}\right)^3 \approx \frac{\eta_s N^3 b^3}{kTn^2 m_b^{3/2}}\begin{cases}1, & c_e < c < c_b \\ c_b/c, & c_b < c < c_D\end{cases} \quad (2.25)$$

where $c_e = n^4 c_0^*$ is the entanglement concentration. The relaxation time is independent of concentration[11,12] in the string-controlled entangled regime ($c_e < c < c_b$) and decreases with increasing concentration $\tau \sim 1/c$ in the bead-controlled regime (see Figure 5).

The self-diffusion coefficient

$$D \approx \frac{R^2}{\tau} \approx \frac{kT}{\eta_s b}\frac{n^2 m_b^{3/2}}{N^2}\begin{cases}(c_b/c)^{1/2}, & c_e < c < c_b \\ (c/c_b)^{1/3}, & c_b < c < c_D\end{cases} \quad (2.26)$$

decreases with concentration in the entangled string-controlled regime, but increases with concentration in the bead-controlled regime (see Figure 6).

The modulus G of entangled polymers is on the order of thermal energy kT per entanglement strand

$$G \approx \frac{kT}{a^2\xi} \approx \frac{kT}{n^2 m_b^{3/2} b^3}\begin{cases}(c/c_b)^{3/2}, & c_e < c < c_b \\ c/c_b, & c_b < c < c_D\end{cases} \quad (2.27)$$

and viscosity

$$\eta \approx G\tau \approx \frac{\eta_s N^3}{n^4 m_b^3}\begin{cases}(c/c_b)^{3/2}, & c_e < c < c_b \\ 1, & c_b < c < c_D\end{cases} \quad (2.28)$$

The viscosity of entangled solutions increases with concentration $\eta \sim c^{3/2}$ in the string-controlled regime but is concentration-independent in the bead-controlled regime (Figure 7).

Note that for the solution to be entangled we need $c_e < c_b$, which implies that $\alpha \equiv N/(n^2 m_b) > 1$. The parameter α is the ratio of the number of beads on the necklace N/m_b to the number of correlation volumes per entanglement strand n^2. If $\alpha < 1$ the chain stays unentangled up to concentration c_D.

The two situations (for $\alpha < 1$ and for $\alpha > 1$) are sketched in Figures 5−7 for relaxation time, self-diffusion coefficient, and viscosity. In the unentangled case the viscosity plateau is at $\eta \approx \eta_s n^2 \alpha$ (for $\alpha < 1$). For the entangled case it is at $\eta \approx \eta_s n^2 \alpha^3$ (for $\alpha > 1$).

3. Effects of Added Salt

The generalization of our model to the case of salt solutions is straightforward.[12] The screening length in the absence of added salt is assumed to be equal to the correlation length ξ (see eqs 2.14 and 2.18 in the string-controlled and the bead-controlled regimes). We assume that the crossover to the higher salt regimes occurs at the ionic strength of the salt equal to the ionic strength of the counterions (for monovalent salt at $fc \approx 2c_s$ where c_s is the salt concentration) (see ref 12 for details). Therefore the screening length for general salt concentrations is obtained from the equations 2.14 and 2.18 by replacing c by $c(1 + 2c_s/fc)$ which gives the screening length in the string-controlled regime

$$r_{scr} \approx b m_b^{1/4} (cb^3)^{-1/2}\left(1 + \frac{2c_s}{fc}\right)^{-1/2} \quad (3.1)$$

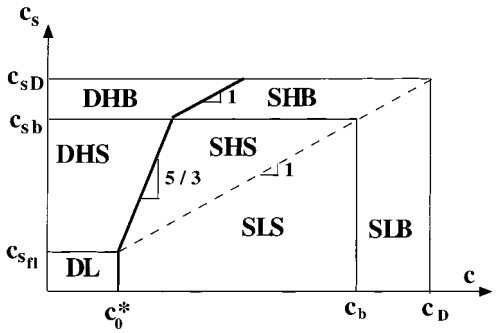

Figure 8. Diagram of regimes for solutions of hydrophobic polyelectrolytes. The thick solid line separates the dilute from the semidilute regime. The dashed line $c_s = fc/2$ separates high-salt from low-salt regimes. DL is the dilute low salt regime. DHS is the dilute high-salt string-controlled regime. DHB is the dilute high-salt bead-controlled regime. SHS is the semidilute high-salt string-controlled regime. SHB is the semidilute high-salt bead-controlled regime. SLS is the semidilute low-salt string-controlled regime. SLB is the semidilute low-salt bead-controlled regime. Both axes are logarithmic.

and in the bead-controlled regime

$$r_{scr} \approx m_b^{1/3} c^{-1/3} \left(1 + \frac{2c_s}{fc}\right)^{-1/3} \tag{3.2}$$

At high salt concentrations ($c_s \gg fc$) the screening length in the string-controlled regime is

$$r_{scr} \approx b m_b^{1/4} \left(\frac{f}{c_s b^3}\right)^{1/2} \tag{3.3}$$

and in the bead-controlled regime it is

$$r_{scr} \approx \left(\frac{m_b f}{c_s}\right)^{1/3} \tag{3.4}$$

Figure 8 shows the diagram of regimes for the solutions of hydrophobic polyelectrolytes as a function of polymer and salt concentrations. The thick solid line corresponds to the overlap concentration separating dilute from semidilute regimes. The dashed line separates high-salt from low-salt regimes. Below we describe each new regime in detail.

Dilute Low-Salt Regime (DL). The chain is in the strongly extended rodlike (or shish kebab like) conformation as long as the screening length r_{scr} is larger than the length of the necklace L_{nec}. The solution is dilute as long as the distance between chains

$$R_{cm} \approx (c/N)^{-1/3} \tag{3.5}$$

is larger than the chain size L_{nec}. The chain becomes flexible when the screening length r_{scr} (eq 3.1) is smaller than the chain size L_{nec} (eq 2.12). (Note that we assume that persistence length is on the order of electrostatic screening length.) This condition gives the following equation for the boundary of the dilute low-salt regime (DL)

$$c_{s_{fl}} \approx \frac{fc}{2}\left(\frac{c_0^*}{c} - 1\right) \tag{3.6}$$

where c_0^* is the overlap concentration in the absence of added salt (eq 2.13). In very dilute solutions ($c \ll c_0^*$) the boundary is at $c_{s_{fl}} \approx fc_0^*/2$.

Dilute High-Salt String-Controlled Regime (DHS). At salt concentrations higher than $c_{s_{fl}}$ the chain is still in the shish kebab like conformation on smaller length scales (less than r_{scr}). On the length scales larger than the screening length r_{scr} (eq 3.1) the statistics of a chain is that of self-avoiding walk of size

$$R \approx r_{scr}^{2/5} L_{nec}^{3/5} \approx b \frac{N^{3/5}}{m_b^{1/5}} \left(cb^3 \left(1 + \frac{2c_s}{fc}\right)\right)^{-1/5} \tag{3.7}$$

In the very high salt dilute ($c_s \gg fc$) string-controlled regime the chain size is $R \approx bN^{3/5}(m_b c_s b^3/f)^{-1/5}$. The macromolecules still do not overlap ($R_{cm} > R$) in the DHS regime.

Dilute High-Salt Bead-Controlled Regime (DHB). The screening length r_{scr} is of the order of the string length $l_{str} \approx b m_b^{1/2}$ between two neighboring beads at salt concentration

$$c_{sb} \approx \frac{fc}{2}\left(\frac{1}{m_b^{1/2} cb^3} - 1\right) \tag{3.8}$$

At high salt concentrations ($c_s \gg fc$) this condition becomes $c_{sb} \approx fc_b/2$, where c_b is the cross-over concentration between semidilute low-salt string-controlled (SLS) and bead-controlled (SLB) regimes (eq 2.16). The size of a chain in the bead-controlled regime at higher salt concentrations is

$$R \approx r_{scr}\left(\frac{N}{m_b}\right)^{3/5} \approx \frac{N^{3/5}}{m_b^{4/15}} \left(c\left(1 + \frac{2c_s}{fc}\right)\right)^{-1/3} \tag{3.9}$$

In the very high-salt ($c_s \gg fc$) dilute bead-controlled regime the chain size is $R \approx bN^{3/5}(c_{sb}/c_s)^{1/3}/m_b^{1/10}$.

Semidilute High-Salt String-Controlled Regime (SHS). In the string-controlled regime the chains overlap and form a semidilute solution of flexible chains when chain size (eq 3.7) is on the order of the distance between chains R_{cm} (eq 3.5). The relation between salt and polymer concentration at chain overlap c^* is

$$c_s \approx \frac{fc^*}{2}\left(\left(\frac{c^*}{c_0^*}\right)^{2/3} - 1\right) \tag{3.10}$$

where c_0^* is the overlap concentration in the low salt regime (eq 2.13). In the very high salt regime ($c_s \gg fc$) the overlap concentration is $c^* = (c_s c_0^{*2/3}/f)^{3/5}$.

The correlation length in the semidilute solution with added salt can be obtained from the general scaling assumption

$$\xi(c) \approx R(c)\left(\frac{c(1 + 2c_s/fc)^{-3/2}}{c^*(1 + 2c_s/fc^*)^{-3/2}}\right)^{-m} \tag{3.11}$$

where one must choose m in such a way that the correlation length ξ is independent of the degree of polymerization N. The exponent is $m = 3/10$ and the correlation length is

$$\xi \approx b m_b^{1/4} (cb^3)^{-1/2} \left(1 + \frac{2c_s}{fc}\right)^{1/4} \tag{3.12}$$

In the semidilute string-controlled regime(SLS) we recover eq 2.14 in the low salt limit ($c_s \ll fc$). In the SHS

regime the correlation length is $\xi \approx b(m_b c_s b^3/f)^{1/3}(cb^3)^{-3/4}$ in the high salt limit ($c_s \gg fc$).

The semidilute polyelectrolyte is a random walk of N/g correlation blobs of size ξ that are space-filling ($c \approx g/\xi^3$) with the chain size

$$R \approx bN^{1/2}\left(\frac{c_b}{c}\right)^{1/4}\left(1+\frac{2c_s}{fc}\right)^{-1/8} \tag{3.13}$$

This crossover relation leads to eq 2.19 at very low salt concentrations ($c_s \ll fc$). At very high salt concentration ($c_s \gg fc$) the chain size is $R \approx bN^{1/2}(m_b c b^3 c_s b^3/f)^{-1/8}$.

Semidilute High-Salt Bead-Controlled Regime (SHB). In the high-salt bead-controlled regime the chains start to overlap at $R \approx R_{cm}$ where the size of the chain R is given by eq 3.9 and the distance between chains is given by eq 3.5. The system crosses over from the dilute bead-controlled regime (DHB) to the semidilute bead-controlled regime (SHB) at overlap concentration

$$c^* \approx \frac{2c_s}{f\left(\left(\frac{N}{m_b}\right)^{4/5}-1\right)} \tag{3.14}$$

Using the general scaling assumption for the correlation length

$$\xi(c) \approx R(c)\left(\frac{1+2c_s/fc}{1+2c_s/fc_*}\right)^m \tag{3.15}$$

where $R(c)$ is given by (eq 3.9) we find

$$\xi \approx m_b^{1/3}c^{-1/3}\left(1+\frac{2c_s}{fc}\right)^{5/12} \tag{3.16}$$

For the semidilute low-salt bead-controlled regime (SLB), we recover eq 2.18 for the correlation length. In the very high-salt ($c_s \gg fc$) semidilute bead-controlled regime the correlation length is $\xi \approx bm_b^{1/2}(c_b/c)^{1/3}(2c_s/fc)^{5/12}$.

The size of a chain in the bead-controlled semidilute solution is

$$R \approx bN^{1/2}\left(\frac{c_b}{c}\right)^{1/3}\left(1+\frac{2c_s}{fc}\right)^{-5/24} \tag{3.17}$$

In the low-salt limit it reduces to eq 2.19. In the high-salt limit ($c_s \gg fc$) the chain size is $R \approx bN^{1/2}(c_b/c)^{1/3}(fc/2c_s)^{5/24}$. Note that the crossover salt concentration separating the string-controlled and the bead-controlled regimes is c_{s_b} (eq 3.8).

We can express any property X of a hydrophobic polyelectrolyte solution with added monovalent salt of concentration c_s in terms of the same property X_0 in the salt-free solution using the scaling relation

$$X = X_0\left(1+\frac{2c_s}{fc}\right)^{\alpha} \tag{3.18}$$

The scaling relations for various properties are listed in Table 1. For solutions with higher concentration of salt our predictions reduce to those for uncharged polymers. It is interesting to note that the results for the salt solutions can be obtained from the ones for the salt-free solutions by substituting m_b by $m_b(1+2c_s/fc)$ in the string-controlled regime and by $m_b(1+2c_s/fc)^{5/4}$ in the bead-controlled regime.

Table 1. Scaling Relations for Semidilute Solutions of Hydrophobic Polyelectrolytes[a]

String-Controlled Regimes
$R = bN^{1/2}m_b^{-1/8}y^{-1/8}(cb^3)^{-1/4}$
$\xi = bm_b^{1/4}y^{1/4}(cb^3)^{-1/2}$

	SHS (unentangled)	SHS (entangled)
τ	$(\eta_s b^3/kT)N^2 m_b^{-3/4}y^{-3/4}(cb^3)^{-1/2}$	$(\eta_s N^3 b^3/kTn^2)m_b^{-3/2}y^{-3/2}$
G	$(kT/N)c$	$(kT/n^2b^3)m_b^{-3/4}y^{-3/4}(cb^3)^{3/2}$
η	$\eta_s N m_b^{-3/4}y^{-3/4}(cb^3)^{1/2}$	$\eta_s(N^3/n^4)m_b^{-9/4}y^{-9/4}(cb^3)^{3/2}$

Bead-Controlled Regimes
$R = N^{1/2}m_b^{-1/6}y^{-5/24}c^{-1/3}$
$\xi = m_b^{1/3}y^{5/12}c^{-1/3}$

	SHB (unentangled)	SHB (entangled)
τ	$(\eta_s/kT)N^2 m_b^{-1}y^{-5/4}c^{-1}$	$(\eta_s N^3/kTn^2)m_b^{-2}y^{-5/2}c^{-1}$
G	$(kT/N)c$	$(kT/n^2)m_b^{-1}y^{-5/4}c$
η	$\eta_s N m_b^{-1}y^{-5/4}$	$\eta_s(N^3/n^4)m_b^{-3}y^{-15/4}$

[a] $y = 1 + 2c_s/fc$, and $m_b \approx \tau/uf^2$ is the number of monomers in a bead.

4. Counterion Condensation

The strong electrostatic attraction between charged groups on the chains and counterions results in counterion condensation. The crossover condition between free and condensed counterions can be found by comparing the entropic loss due to localization of the counterions with the electrostatic interaction between a counterion and the charges on the chain.

Condensation on Strings. For long linear strings we recover the classical Manning condition[15] that the linear line density of charges is less than or equal to one per Bjerrum length (for monovalent counterions)

$$f\frac{g_T}{\xi_T} \approx \frac{f}{b\tau} \le \frac{1}{l_B} \tag{4.1}$$

where ξ_T and g_T are the size and the number of monomers in the thermal blob (see eq 2.4). Thus there is no counterion condensation on linear strings between beads if

$$f < \frac{\tau}{u} \tag{4.2}$$

Otherwise counterions condense to reduce the charge density on the strings to the effective one

$$(f_{str})_{eff} = \frac{\tau}{u} \tag{4.3}$$

Stability of Beads. The charged beads are stable with respect to counterion condensation as long as the electrostatic interaction between a bead and a counterion on its surface is smaller than the thermal energy kT

$$\frac{e^2Q_b}{\epsilon D_b} < kT \tag{4.4}$$

where eQ_b is the charge and D_b is the size of a bead

(see section 2.2). This leads to the condition on the number of monomers on a bead

$$Q_b < \frac{D_b}{l_B} \tag{4.5}$$

From the Rayleigh stability condition for a bead

$$l_B \frac{Q_b^2}{D_b} \approx \frac{D_b^2}{\xi^2} \tag{4.6}$$

we obtain

$$Q_b^2 \approx \frac{D_b^3 \tau^2}{l_B b^2} \tag{4.7}$$

Combining eqs 4.5 and 4.7, we obtain the stability condition for a bead with respect to counterion condensation

$$D_b < \frac{b}{u\tau^2} \tag{4.8}$$

Using the relation between the size D_b and the number of monomers m_b in a bead (eq 2.3) $D_b \approx b(m_b/\tau)^{1/3}$ we can rewrite the inequality (eq 4.8) as

$$m_b < \frac{1}{u^3\tau^5} \tag{4.9}$$

It is important to stress that the relations 4.4−4.9 are general and do not depend on the charge distribution inside the beads. Note that smaller beads (eqs 4.8 and 4.9) are stable against counterion condensation. From the Rayleigh condition, it follows that smaller beads correspond to larger fractional charge f (see eq 2.9). Thus weakly charged hydrophobic polyelectrolytes (low f) with large beads are unstable against counterion condensation. For the uniformly charged beads, the condition of bead stability can be expressed in terms of fractional charge

$$u\tau^3 < f \leq 1 \tag{4.10}$$

where we have not included numerical prefactor at the lower bound. Hydrophobic polyelectrolytes with lower fractional charge $f < u\tau^3$ do not form stable necklaces, but rather collapse into globules due to counterion condensation and precipitate from solution. Similar instability was predicted for cylindrical globules.[8] In other words, inequality 4.10 is the condition for solubility of hydrophobic polyelectrolytes.

Condensation on Necklaces. In addition to counterion condensation on strings (controlled by the linear charge density on the strings) and on spherical beads (controlled by the charge and the size of the beads) one needs to consider condensation on the necklace controlled by its total charge. At distances from the necklace larger than l_{str} but smaller than L_{nec} the electric field has cylindrical symmetry and counterion condensation is determined by the total charge (of beads and strings) of the necklace. The linear density can be approximated by the charge of the beads spread over the length of the strings fm_b/l_{str}. The necklace is stable with respect to counterion condensation if the Manning condition[15] (see eq 4.1) is satisfied

$$f\frac{m_b}{l_{str}} \approx \frac{1}{b}\left(\frac{\tau}{u}\right)^{1/2} < \frac{1}{l_B} \tag{4.11}$$

This stability condition can be rewritten as

$$\tau u < 1 \tag{4.12}$$

If this condition is not satisfied, counterions are localized within distance l_{str} of the necklace and screen the repulsion between beads, leading to the collapse of the necklace into a globule and precipitation from solution. Note that inequality 4.12 is independent of the fraction of charged monomers f.

Surface Charges. Another effect that has been ignored above is the decrease of the dielectric constant due to high polymer density inside the beads. This lower dielectric constant causes counterions to condense in the core of the beads leaving the charges only in the thin layer near the surface. The thickness of this layer is determined by the specifics of the local interaction between the water molecules and dissociated charged groups on the polymer chain. For simplicity we can assume this charged shell to be of thickness ξ_T—the size of the thermal blob. The number of thermal blobs in this charged shell is $\approx(D_b/\xi)^2$ and the number of monomers in each thermal blob is $\approx(\xi/b)^2$. Therefore, there are $(D_b/b)^2$ monomers in the charged shell with the charge of the bead

$$f\left(\frac{D_b}{b}\right)^2 \approx f\left(\frac{m_b}{\tau}\right)^{2/3} \tag{4.13}$$

where we have used eq 2.3 relating the size and the degree of polymerization of beads. The Rayleigh's stability condition for beads with charged shells is (see eq 4.7)

$$f^2\left(\frac{m_b}{\tau}\right)^{4/3} \approx \frac{D_b^3\tau^2}{l_B b^2} \approx \frac{m_b}{u\tau} \tag{4.14}$$

where we have used eq 2.3 in the last part of the above equation. From eq 4.14 we find the stable number of monomers

$$m_b \approx \frac{\tau^7}{u^3 f^6} \tag{4.15}$$

and the stable size

$$D_b \approx b\frac{\tau^2}{uf^2} \tag{4.16}$$

of the shell-charged beads. The length of the strings is obtained by balancing the repulsion between beads and the surface energy of the strings $(l_B/l_{str})f^2(m_b/\tau)^{4/3} = l_{str}/\xi_T$

$$l_{str} \approx b\frac{\tau^{7/2}}{(uf^2)^{3/2}} \approx b m_b^{1/2} \tag{4.17}$$

The length of the necklace with the surface-charged beads is

$$L_{nec} \approx l_{str}\frac{N}{m_b} \approx b\frac{N(uf^2)^{3/2}}{\tau^{7/2}} \approx b\frac{N}{m_b^{1/2}} \qquad (4.18)$$

Note that the parameters of the necklace with the surface-charged beads (eqs 4.15−4.18) were obtained in a manner analogous to that for the necklace with uniformly charged beads (eqs 2.9, 2.8, 2.10, and 2.12). These results can be easily extended to semidilute solutions of necklaces with surface-charged beads.

The derivation of the onset of counterion condensation for surface-charged beads coincides with that for uniformly charged beads (eqs 4.4−4.9). Substituting the number of monomers in the surface-charged beads (eq 4.15) into inequality 4.9, we obtain the range of stability of these necklaces

$$\tau^2 < f \leq 1 \qquad (4.19)$$

The onset of counterion condensation on the necklace is the same as for uniformly charged beads (inequality 4.12).

5. Comparison with Experiments

The predictions of our model are in semi-quantitative agreement with the scattering experiments of C. Williams' group[16] and F. Boue's group[17] on aqueous solutions of polystyrene sulfonate. They observed that the position of the correlation peak ξ shifts with polymer concentration as $c^{-1/3}$ for weakly charged polymers (partially sulfonated polystyrene) in agreement with our prediction (eq 2.18). The size of the chains R measured by neutron scattering from deuterated samples[17] is larger than correlation length ξ, indicating that $\xi \sim c^{-1/3}$ is observed in semidilute solutions. In this unusual regime the correlation length decreases with increasing charge on the chain as $\xi \sim f^{-0.8\pm0.1}$ not too far from our prediction $\xi \sim f^{-2/3}$ (see eqs 2.18 and 2.9). The form factor has bead-like features with size D_b decreasing with increasing charge f (see our prediction, eq 2.8). Addition of salt decreases chain size (as we predict in eq 3.17) but does not affect the bead size D_b.

It would be interesting to test other predictions of our theory. In particular it is very important to confirm the existence of both string-controlled and bead-controlled regimes for the same polymer. According to our theory, the width of the concentration interval, where the usual polyelectrolytes scaling ($\xi \sim c^{-1/2}$) occurs, is proportional to the square of the number of beads on the chain.

$$\frac{c_b}{c_0^*} \approx \left(\frac{N}{m_b}\right)^2 \approx N_{bead}^2 \qquad (5.1)$$

The increase of the number of the charged groups on a chain results in the increase of the number of beads (and the decrease of their size) and in the opening of the window of the classical polyelectrolyte behavior $\xi \sim c^{-1/2}$.

We would like to point out the similarity between some of our predictions and the recent experimental observations of Boris and Colby for sulfonated polystyrene.[18] They have noticed a regime with concentration dependence of semidilute solution viscosity weaker than predicted by the Fuoss law (unentangled string-controlled regime) $\eta \sim c^{1/2}$ (see the $c < c_b$ part of eq 2.24). In the same range of polymer concentrations, they observed reciprocal critical shear thinning rate (which they interpreted as a relaxation time τ) to decrease with increasing polymer concentration as $\tau \sim c^{-0.9}$ is much stronger than predicted for the Rouse string-controlled unentangled regime $\tau \sim c^{-0.5}$ (see the $c < c_b$ part of eq 2.22). These observations are consistent with the trend predicted by our bead-controlled regime (see the $c > c_b$ parts of eqs 2.22 and 2.24). Note also that there is no analogous anomaly in hydrophilic polyelectrolytes in similar concentration regimes that points out the hydrophobic nature of this phenomena. Of course, these similarities could be fictitious and more detailed experimental tests are needed to validate our scaling model.

Acknowledgment. This work was supported in part by the National Science Foundation (through Grants DMR-9696081 and DMR-9730777) and by the Eastman Kodak Company. M.R. would like to acknowledge discussions with C. Williams and W. Essafi and the hospitality of the Laboratoire de Physique de la Matiere Condensee at the College de France where part of this manuscript was written.

References and Notes

(1) *Polyelectrolytes*; Hara, M., Ed.; Marcel Dekker: New York, 1993.
(2) Tanford C. *Physical Chemistry of Macromolecules*; Wiley: New York, 1961.
(3) Rayleigh, Lord *Philos. Mag.* **1882**, *14*, 182.
(4) Kantor, Y.; Kardar, M. Europhys. Lett. **1994**, *27*, 643.
(5) Kantor, Y.; Kardar, M. Phys. Rev. E **1995**, *51*, 1299.
(6) Dobrynin, A. V.; Rubinstein, M.; Obukhov, S. P. *Macromolecules* **1996**, *29*, 2974.
(7) Grosberg, A. Yu.; Khokhlov, A. R. *Statistical Physics of Macromolecules*; AIP Press: New York, 1994.
(8) Khokhlov, A. R. *J. Phys. A* **1980**, *13*, 979.
(9) de Gennes, P. G. *Scaling Concepts in Polymer Physics*; Cornell University Press: Ithaca, NY, 1979.
(10) de Gennes, P.-G.; Pincus, P.; Velasco, R. M.; Brochard, F., *J. Phys. (Paris)* **1976**, *37*, 1461.
(11) Rubinstein, M.; Colby, R. H.; Dobrynin, A. V. *Phys. Rev. Lett.* **1994**, *73*, 2776.
(12) Dobrynin, A. V.; Colby, R. H.; Rubinstein, M. *Macromolecules* **1995**, *28*, 1859.
(13) Kavassalis, T. A.; Noolandy, J. *Phys. Rev. Lett.* **1987**, *59*, 2674; *Macromolecules* **1989**, *22*, 2709.
(14) Lin, Y.-H. *Macromolecules* **1987**, *20*, 3080.
(15) Manning, G. S. *J. Chem. Phys.* **1969**, *51*, 924.
(16) Essafi, W. Ph.D Thesis, Paris, 1996.
(17) Spiteri, M.-N. Ph.D. Thesis, Orsay, 1997.
(18) Boris D.; Colby, R. H. *Macromolecules*, submitted for publication.

MA981412J